

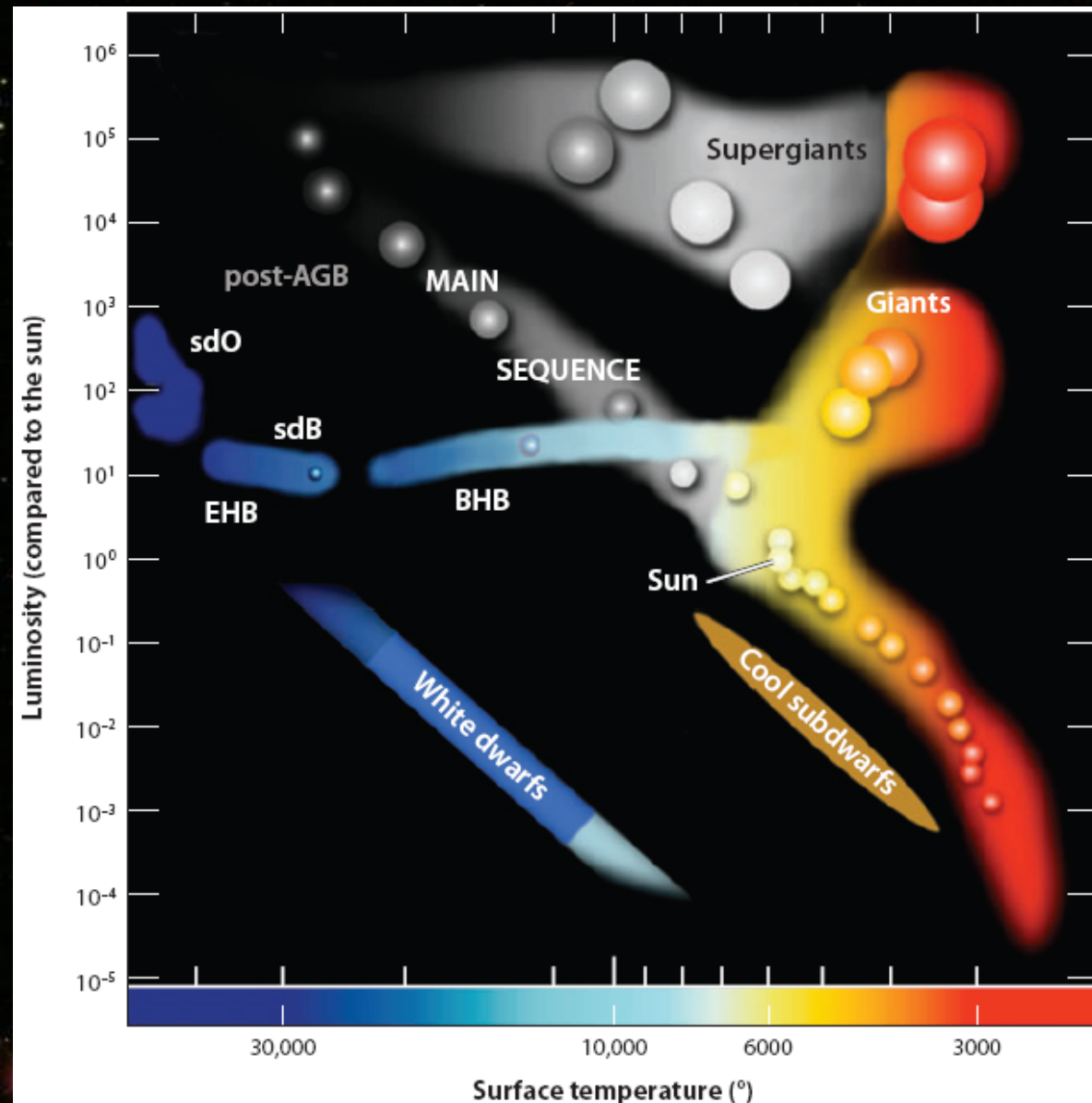
Observational Asteroeismology of Hot Subdwarf Stars

Roy H. Østensen
KU Leuven, Belgium

Summary

- * **Where do hot subdwarf stars come from?**
 - * Binary formation channels
 - * Merger channels
- * **Pulsational properties of hot subdwarfs**
 - * *p*-mode pulsators
 - * *g*-mode pulsators
- * **Observational techniques**
 - * Frequency analysis
 - * Multi-colour photometry
 - * Spectroscopy
- * **Recent results**

Extreme Horizontal Branch



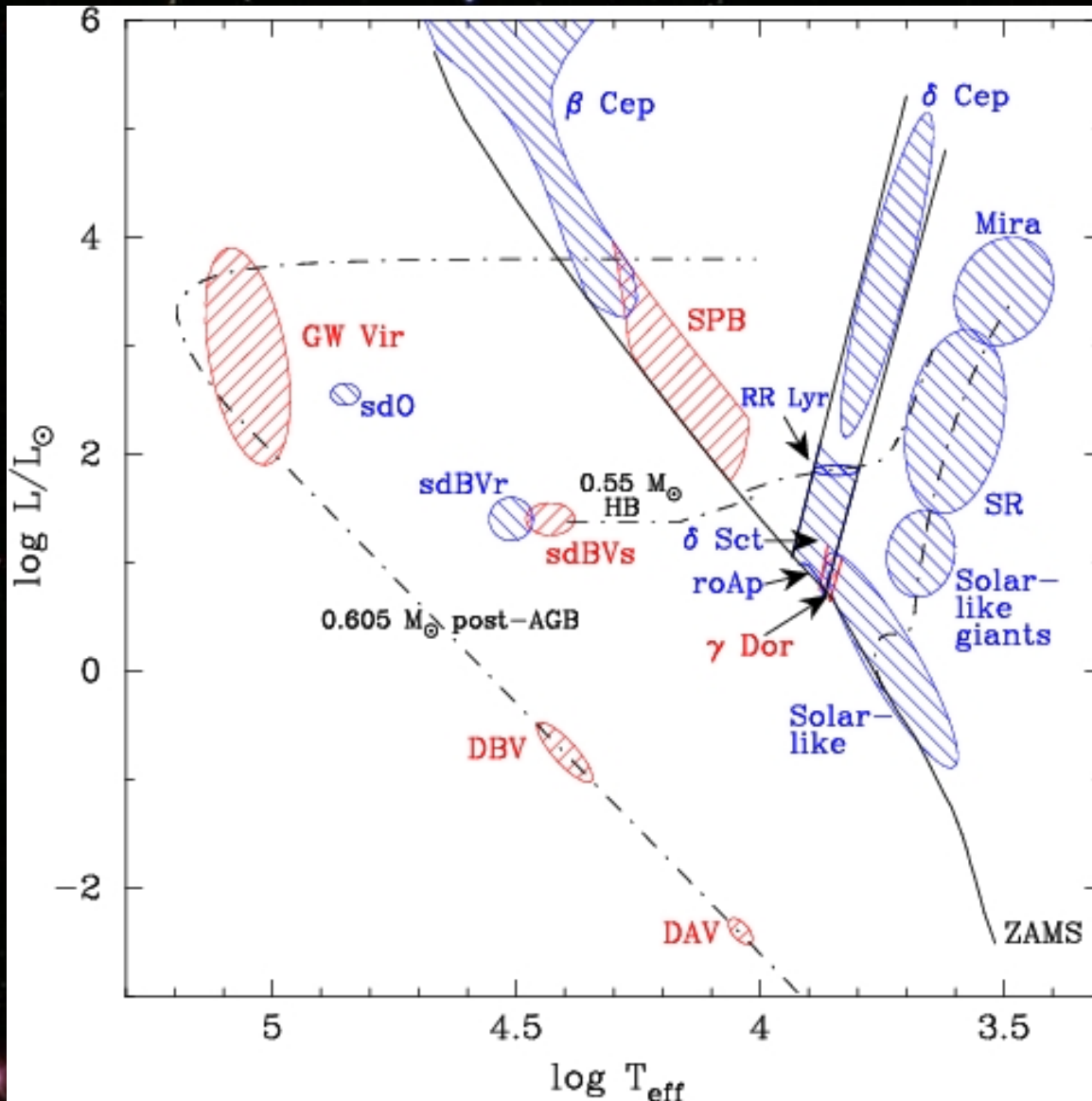
sdB and sdO stars discovered in blue stars surveys

Heber (1986) identifies the EHB stars as 0.5 solar mass core-helium burning post-RGB stars, with envelopes too thin to sustain shell-hydrogen burning

The sdB stars evolve into sdO stars after the helium in the core is burnt. After the short-lived shell-helium burning period, they go directly to the white dwarf cooling track, without ever becoming AGB stars

Fig: Heber (2009)

Extreme Horizontal Branch



Both sdB and sdO stars show pulsations excited by the the same Z-bump driven kappa-mechanism that operates in beta Cep and SPB stars

Blue: p-mode pulsators:

sdBVr = 'rapid' pulsations

P = 60-600s

Red: g-mode pulsators

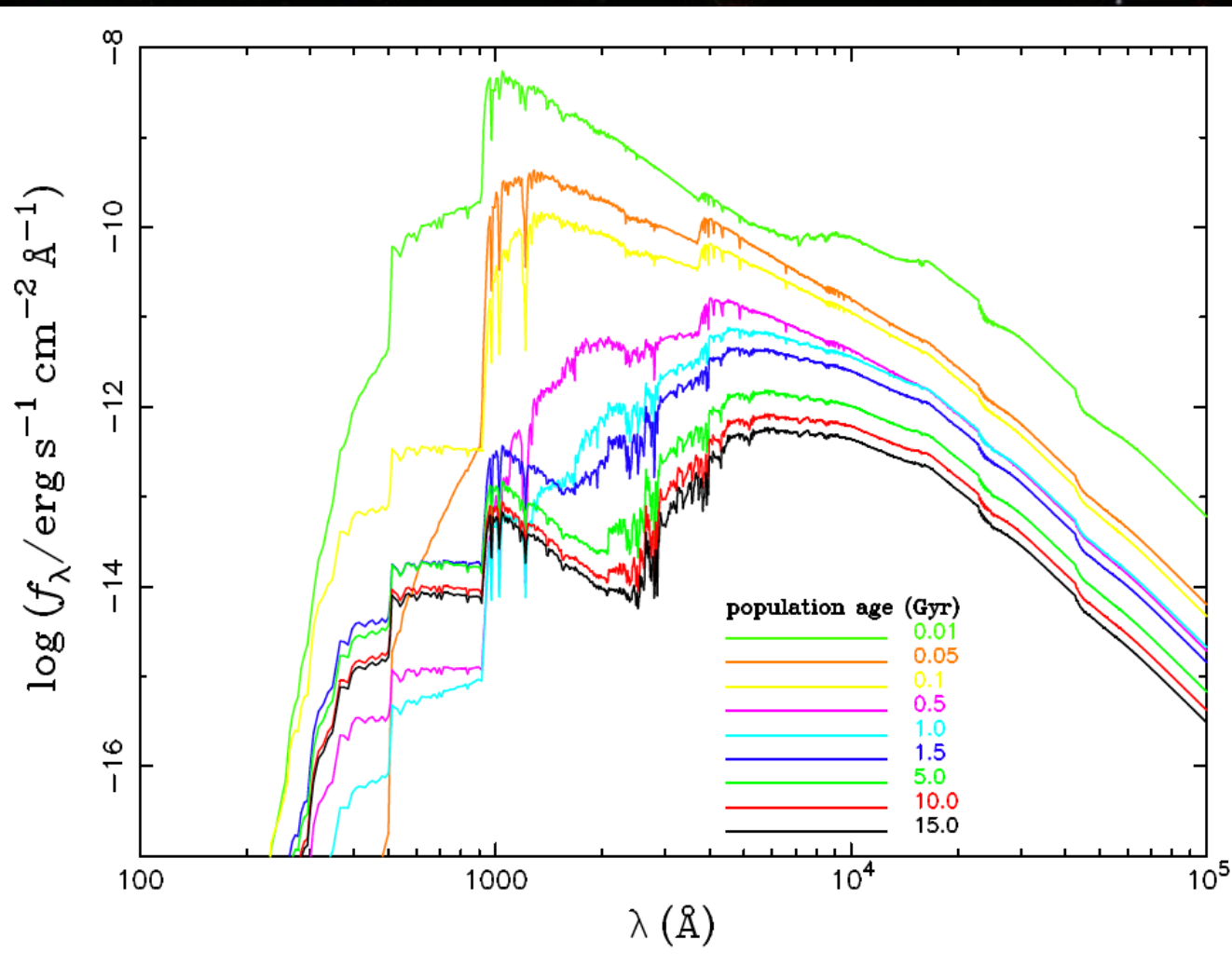
sdBVs = 'slow' pulsations

P = 1800-18000s

Asteroseismic HR diagram;

Adopted from J. Christensen-Dalsgaard

The UV upturn phenomenon



The FUV spectrum of elliptical galaxies resembles model spectra of EHB stars

At least 4 channels are required to explain the observed populations (Han et al. 2002,2003)

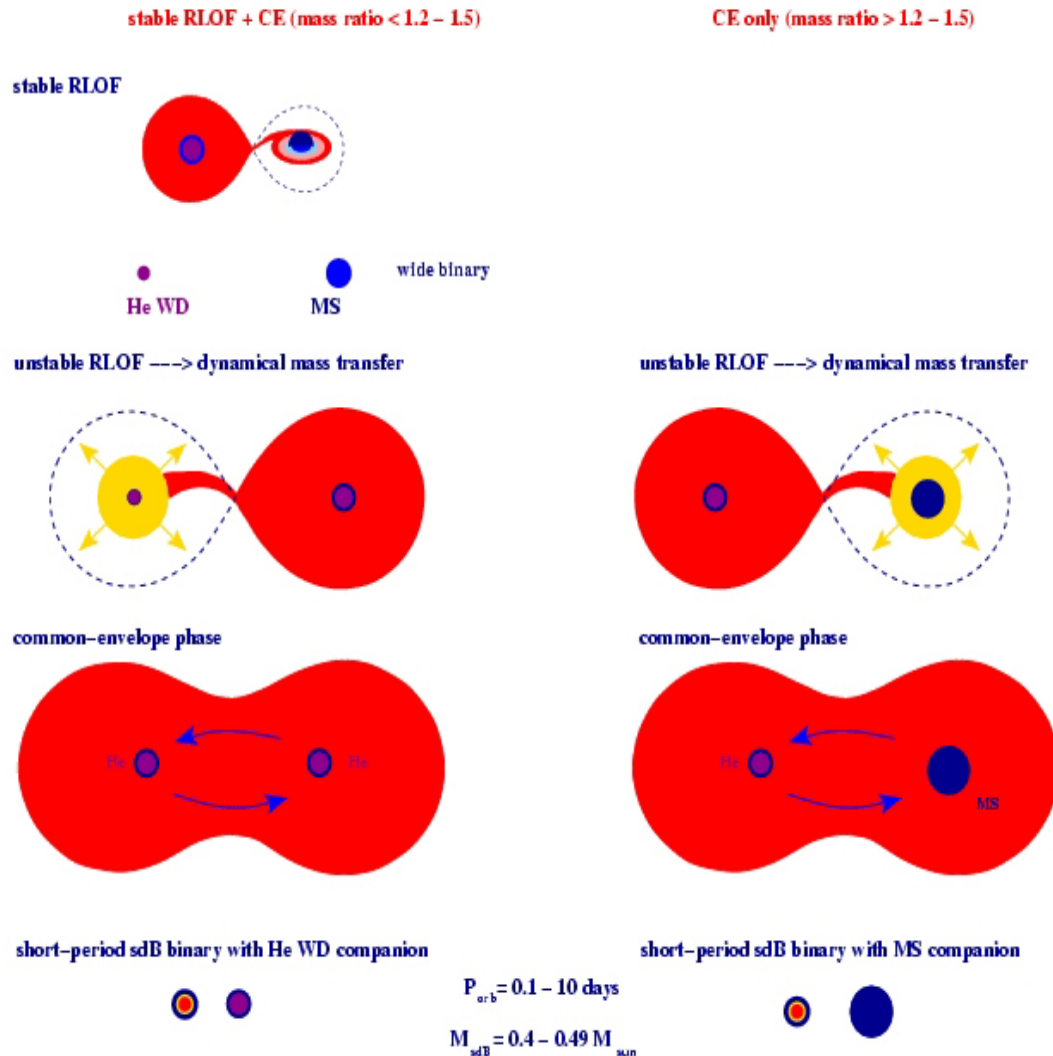
EHB stars dominate the UV flux after 1.1Gyr

Canonical sdB theory

- * sdB stars are Extreme Horizontal Branch (EHB) stars, $M \sim 0.5 M_{\odot}$
- * An extremely thin hydrogen envelope – no more than 1% by mass
- * Post RGB stars that have started core helium burning in a Helium flash
- * EHB core He burning phase:
100 – 150 million years
- * Post-EHB shell H & He burning and settling (2 – 20 Myr) take the stars through the sdO domain to the WD cooling curve without any AGB phase
- * Their formation require a particular mechanism to remove the envelope on the RGB:
 - * Common envelope ejection (CEE)
 - * 1) Secondary is a main sequence star
 - * 2) Secondary is a white dwarf
 - * Stable Roche lobe overflow (RLOF)
 - * 1) Secondary is a MS star
 - * 2) Secondary is a WD
- * He-WD + He-WD merger
- * Enhanced wind on the RGB (?)

Common envelope ejection

Common-Envelope Channels



- ★ Low ZAMS mass stars ($1.8 - 2.0 M_{\odot}$), ignite He in a core flash when the core reaches $\sim 0.46 M_{\odot}$
- ★ If the envelope is ejected before the core reaches the flash mass, the core never goes to the EHB.
- ★ More massive stars ignite helium non-degeneratively, before the tip of the RGB. EHB mass $> 0.33 M_{\odot}$

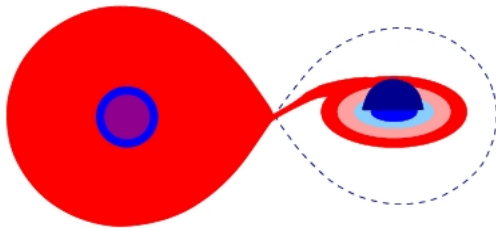
Fig: Podsiadlowzki (2008)

Stable Roche lobe overflow

Stable RLOF Channel

(mass ratio < 1.2 – 1.5)

stable RLOF (near tip of RGB)



wide sdB binary with MS/SG companion



$P_{\text{orb}} = 10 - 500$ days

$M_{\text{sdB}} = 0.30 - 0.49 M_{\text{sun}}$

★ If mass is transferred onto a more massive companion the radius of the orbit will keep increasing without ever producing a CE.

$P \sim 100$ to 2000 days.

★ If the primary has a mass below the helium flash mass, RLOF has to occur close to the tip of the RGB, and the mass distribution is sharp. Otherwise, non-degenerate helium burning starts earlier, and the output is an sdB star with mass between 0.33 and $1.1 M_{\odot}$ (Han, Tout & Eggleton 2000).

★ The core can keep growing while envelope is peeled off

Fig. From Podsiadlowzki (2008): “Hot Subdwarfs in Binaries as the Source of the Far-UV Excess in Elliptical Galaxies”

sdB formation scenarios

Stable RLOF + CE channel
(mass ratio $< 1.2 - 1.5$)

Stable RLOF

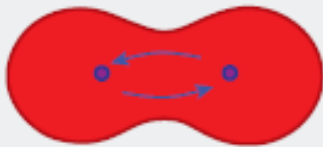


Wide binary

Unstable RLOF



Common envelope



Short-period sdB binary



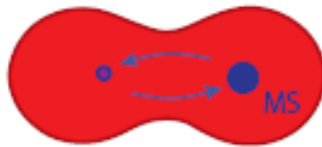
$P_{\text{orb}} = 0.1 - 10$ days
 $M_{\text{sdB}} = 0.40 - 0.49 M_{\odot}$

CE-only channel
(mass ratio $> 1.2 - 1.5$)

Unstable RLOF



Common envelope



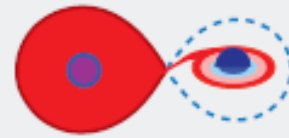
Short-period sdB binary



$P_{\text{orb}} = 0.1 - 10$ days
 $M_{\text{sdB}} = 0.40 - 0.49 M_{\odot}$

Stable RLOF channel
(mass ratio $< 1.2 - 1.5$)

Stable RLOF near tip of RGB



sdB with MS/SG companion



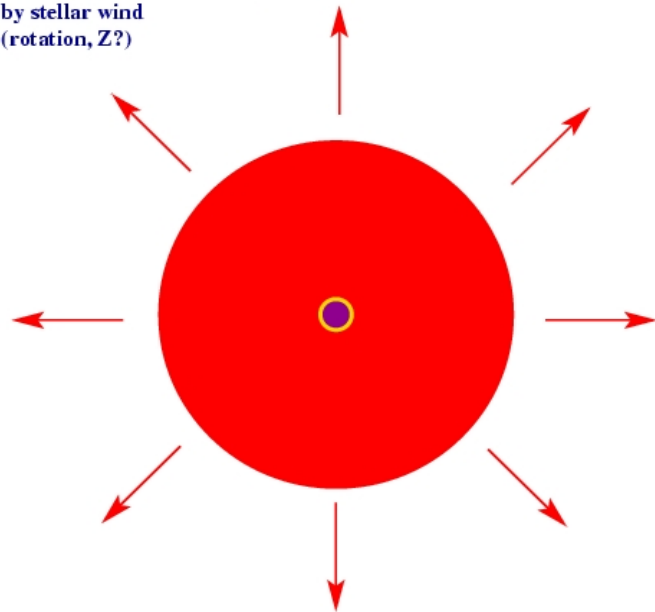
$P_{\text{orb}} = 10 - 500$ days
 $M_{\text{sdB}} = 0.30 - 0.45 M_{\odot}$

Heber (2009)

Single sdB formation

Single sdB Stars

envelope loss near RGB tip
by stellar wind
(rotation, Z?)



$M_{\text{sdB}} = 0.45 - 0.49 M_{\text{sun}}$

He WD merger
(1 or 2 CE phases)



gravitational radiation

$M_{\text{sdB}} = 0.40 - 0.65 M_{\text{sun}}$

A significant number of sdBs are observed as single stars. Their formation is the most problematic and controversial

Proposed scenarios:

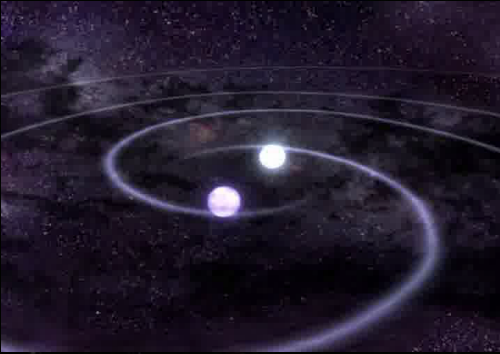
Enhanced stellar wind on the RGB
(D'Cruz et al. 1996)

Merger of two He-core WD stars (Iben 1990, Saio & Jeffery 2000)

CEE by giant planet that evaporates in process (Soker 1998)

Fig. From Podsiadlowski (2008): "Hot Subdwarfs in Binaries as the Source of the Far-UV Excess in Elliptical Galaxies"

He-WD + He-WD mergers



Binaries with 2 He-WD stars can form after 2 CE phases or 1 stable RLOF phase and 1 CE phase

If the orbital period after the final CE phase is short, it will shrink (on a reasonable timescale) due to gravitational wave radiation, and the WDs merge

He-WDs have masses between $0.2 M_{\odot}$ and the He flash mass $\sim 0.46 M_{\odot}$

The end product must therefore have masses between 0.4 and $\sim 0.8 M_{\odot}$

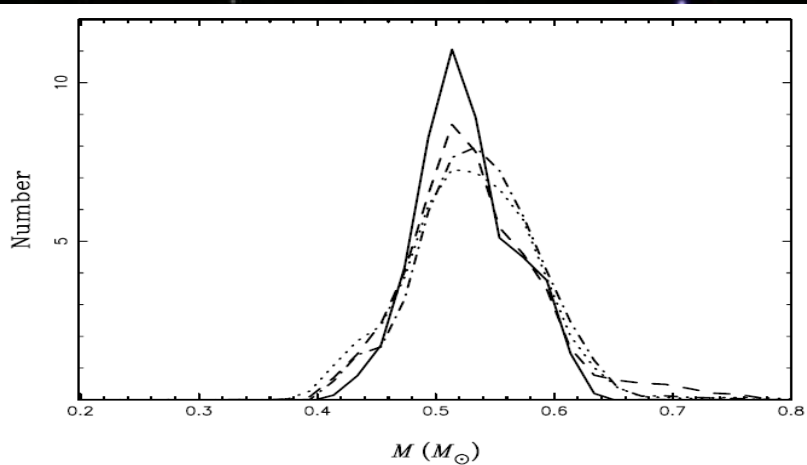


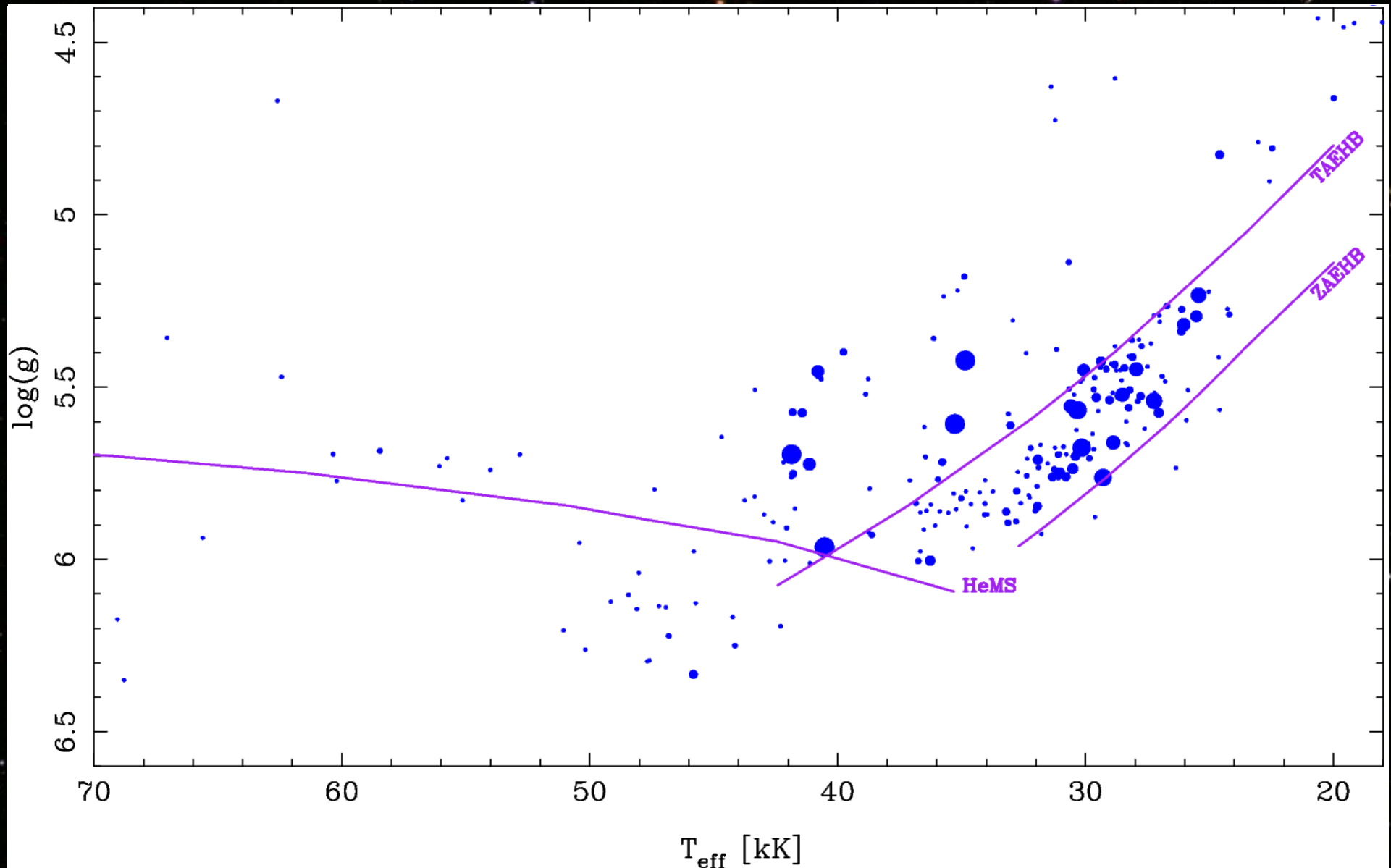
Figure 13. The mass distribution of the He + He WD merger product. Solid, dashed, dot-dashed and dotted curves are for simulation sets 1, 2, 3 and 4, respectively. Simulation set 1 is for $Z = 0.02$, $\alpha_{\text{CE}} = 0.5$, $\alpha_{\text{th}} = 0.5$; simulation set 2 is for $Z = 0.02$, $\alpha_{\text{CE}} = 1.0$, $\alpha_{\text{th}} = 1.0$; simulation set 3 is for $Z = 0.004$, $\alpha_{\text{CE}} = 0.5$, $\alpha_{\text{th}} = 0.5$; simulation set 4 is for $Z = 0.004$, $\alpha_{\text{CE}} = 1.0$, $\alpha_{\text{th}} = 1.0$.

Han et al. (2002)

Surveys for hot subdwarf stars

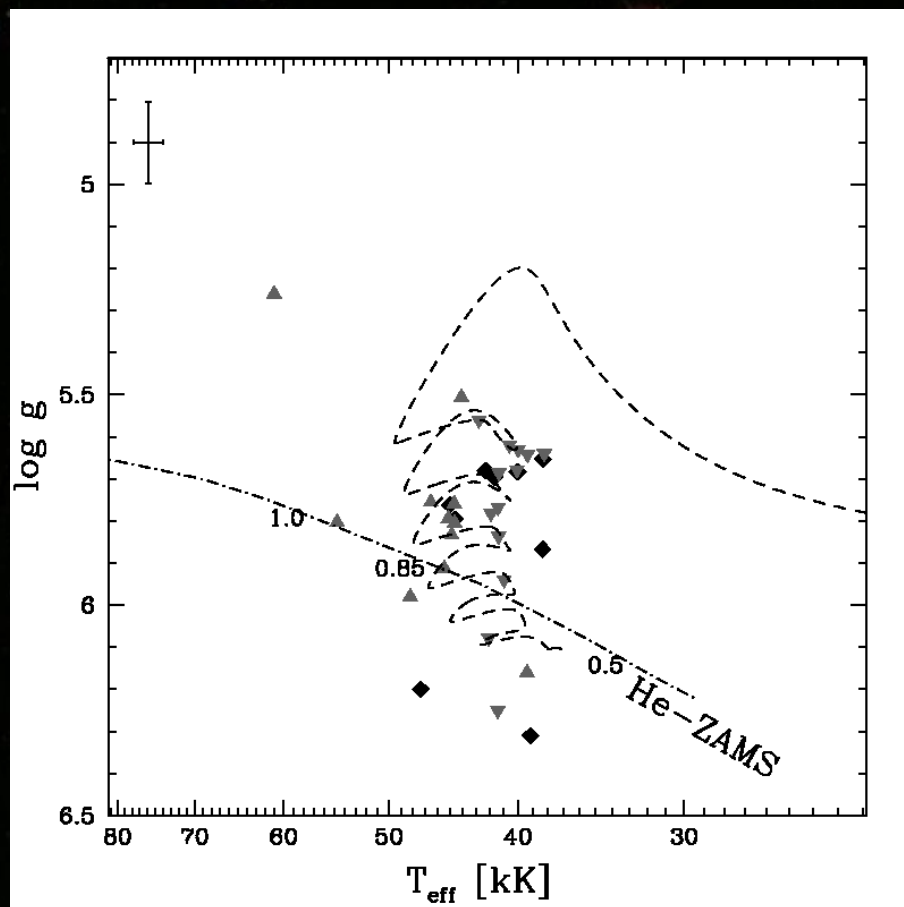
- * Surveys find 1000s of hot subdwarfs in the field
- * PG survey: >1000 hot subdwarfs, dominant population of faint blue stars down to the survey limit ($B=16.5$)
- * SDSS survey: ~1000 hot subdwarfs, but they give way to WDs below $\sim B=18$, where WD stars dominate
- * The Subdwarf Database catalogs 2500 hot subdwarfs
- * Radial Velocity (RV) surveys
- * Maxted et al. (2001), Morales-Rueda et al. (2003, 2006)
- * SPY survey (VLT), Lisker (2005), Ströer (2007)
- * Green et al. (2008), Bright, low-res, uniform
- * Binary fractions
- * 50 – 66 % depending on selection

Spectroscopic surveys



Sample from Green et al (2008) "Systematics of Hot Subdwarfs Obtained from a Large Low Resolution Survey"

Results from the SPY survey



sdB stars from the Supernova 1A Progenitor survey (SPY, Stroer 2006)

Open symbols: He-deficient sdB & sdO stars

Filled symbols: He-enriched sdO stars (CN indicated)

Clearly different populations

Objects below the He-MS indicates that they may not be core He-burning stars

He-deficient sdO stars could be explained by the late hot flasher scenario

Pulsating hot subdwarf stars

- ★ **V361 Hya stars; (Kilkenny et al. 1997)**
 - ★ sdB/sdOB; T_{eff} : 28 – 34.000 K, $\log g$: 5.5 – 6.0, $I=10\%$
 - ★ p -modes; A: 1 – 50 mma, P: 100 – 380s, N = 52
- ★ **V1093 Her stars; (Green et al. 2003)**
 - ★ sdB; T_{eff} : 22 – 28.000 K, $\log g$: 5.1 – 5.6, $I=75\%$
 - ★ g -modes; A: 1 – 2 mma, P \approx 1h, N \approx 50
- ★ **DW Lyn stars; (Schuh et al. 2005)**
 - ★ sdB; $T_{\text{eff}} = 28.000\text{K}$, Hybrid $p+g$ mode pulsators
 - ★ $p+g$ modes; g -modes; N = 5
- ★ **LS IV-14°116 (Ahmad & Jeffery 2005)**
 - ★ He-sdB with $T_{\text{eff}} = 32.500\text{K}$, $\log g = 5.4$
 - ★ A: 10 mma, P \approx 1000s
- ★ **V338 Ser, J20136+0928**
 - ★ sdB; $T_{\text{eff}} = 31 – 33.000$ K, $\log g$: 5.1 – 5.3
 - ★ A: 10 – 50 mma, P: 350 – 600s, N=2
- ★ **J17006+0748, EO Ceti; (Woudt et al. 2006)**
 - ★ sdO+F; $T_{\text{eff}} \approx 60.000$ K, $\log g \approx 5.5$, P \approx 60s!, A \approx 40 mma

Pulsating sd's in binaries

- ★ **V361 Hya stars; N=52**
 - ★ sdB+dM: 1 eclipsing – NY Vir, 2 reflection eff.
 - ★ sdB+WD: 2 (short period post CE)
 - ★ sdB+FGK: 15++ (post RLOF)
- ★ **V1093 Her stars; N~50 (most unconfirmed)**
 - ★ Hard to say due to long periods which are difficult to measure from the ground. Space data solves the problem
- ★ **DW Lyn stars; N=5**
 - ★ 2M1938+4603
 - ★ Most apparently single, according to P-dot measurements
- ★ **V338 Ser, J20136+0928**
 - ★ No sign of companions
- ★ **sdO pulsators; J17006+0748, EO Ceti**
 - ★ sdO+F; (post RLOF)

Properties of V361 Hya stars

49 short period pulsators at the last count

Most are multiperiodic

1/3 in wide binaries with F-G companions

1/10 are in close binaries with dM or WD companions, and showing reflection effects, eclipses and ellipsoidal modulations

>25% show no trace of a stellar companion in RV

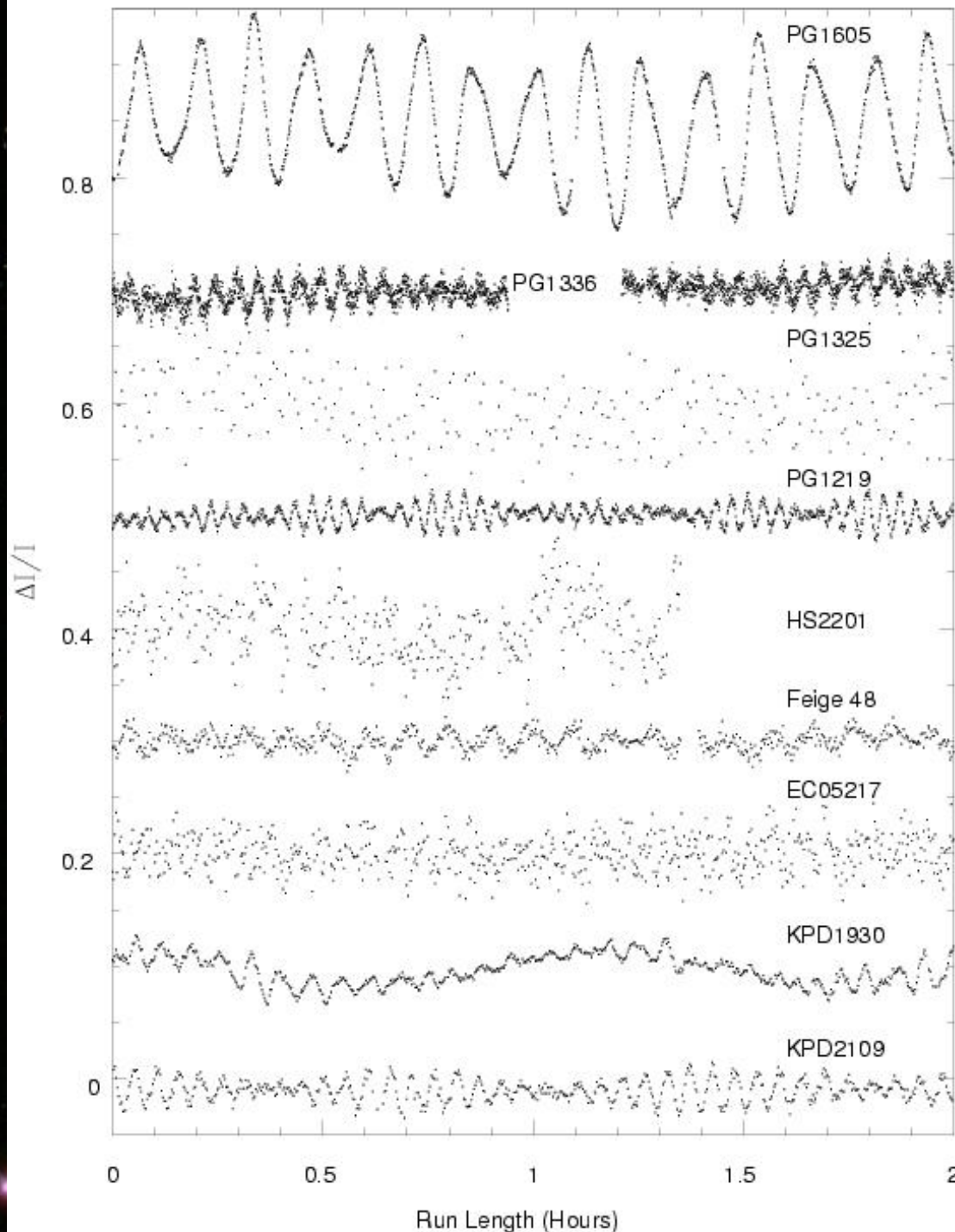
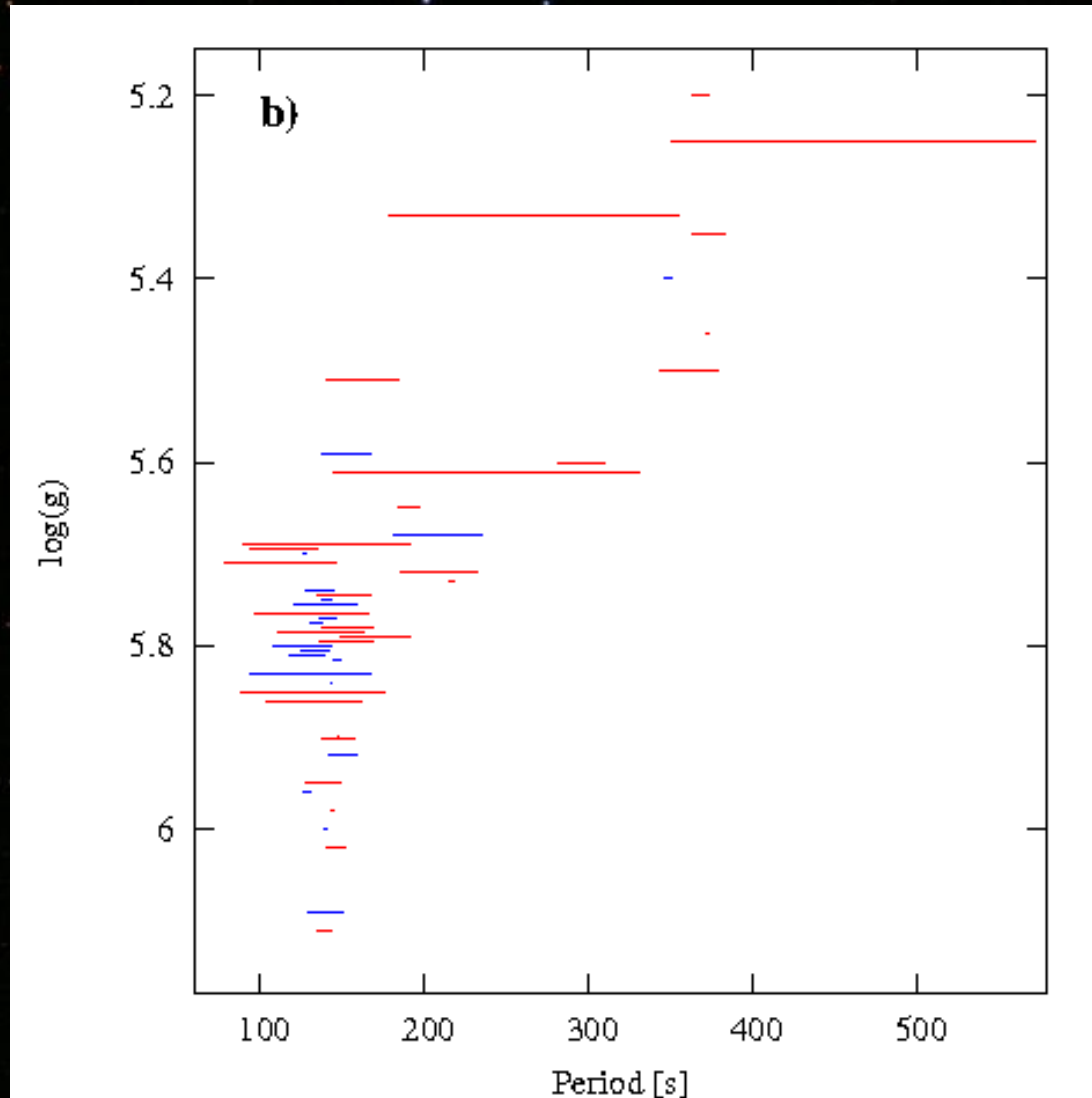


Fig. courtesy M. Reed

Pulsational properties of V361 Hya



The properties of the 49 V361 Hya stars are summarised in Østensen et al. 2010

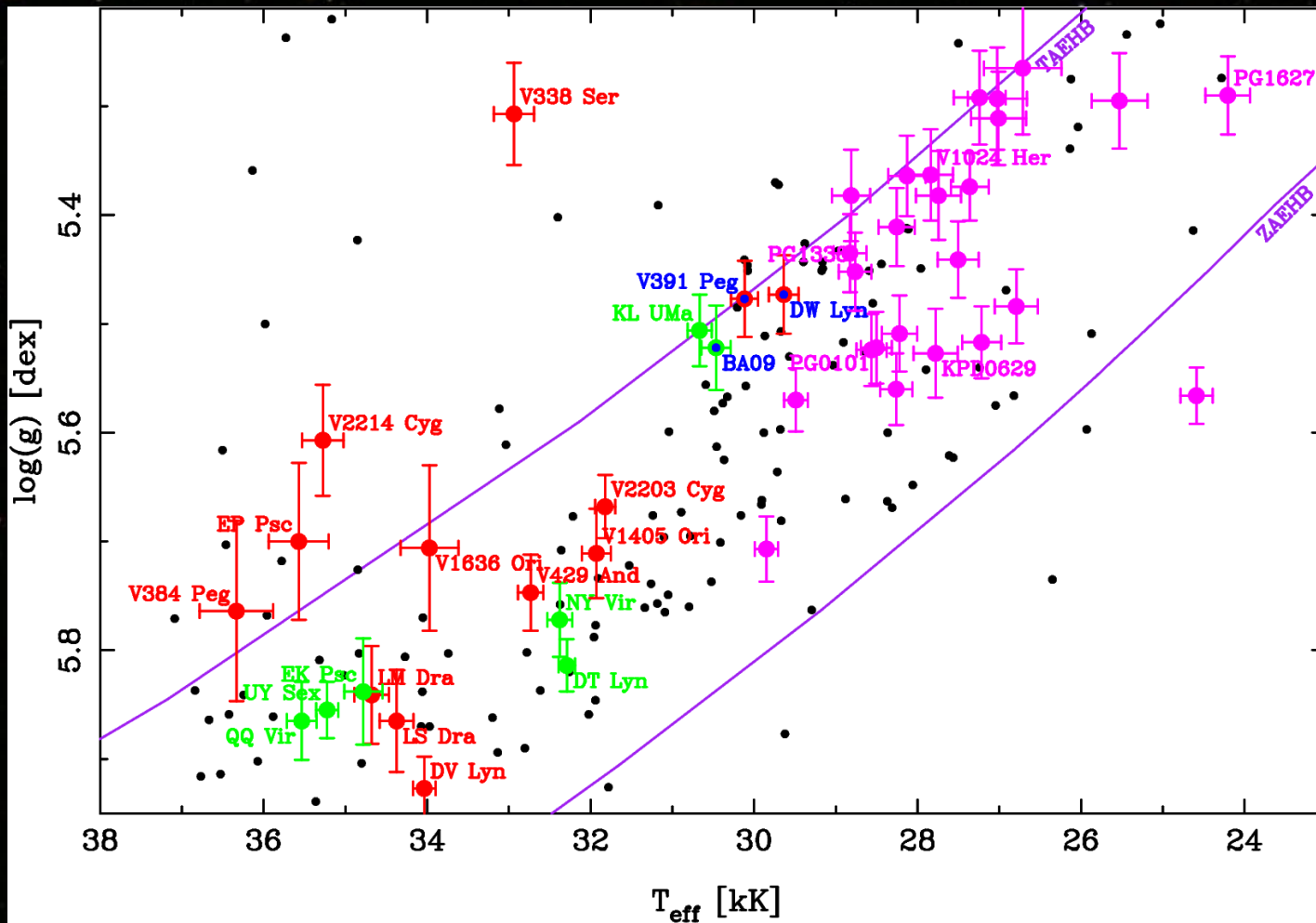
Systematic trends in temperature/gravity relations

High amplitudes are more common in the low-gravity stars, possibly due to radial modes

Period/gravity relationship breaks down for gravities higher than $\log(g) = 5.8$

Figs. from Østensen et al.
2010 (arXiv:1001.3657)

P-modes and g-modes across the Extreme Horizontal Branch



Pulsating EHB stars in the BG sample (consistent high-S/N spectroscopy)
Green: Stars with seismological solutions
Purple: V1024 Her stars
Blue: Hybrid pulsators
Black: Non-pulsators

Fig. from Østensen et al.
2009 (arXiv:0901.1618)

Mode identification

Three methods currently attempted on sdBVs:

- 1) Period matching in white light data
- 2) Spectroscopic mode ID
- 3) Amplitude ratios from multi-color photometry
- 4) Combination method: multi-color + RV

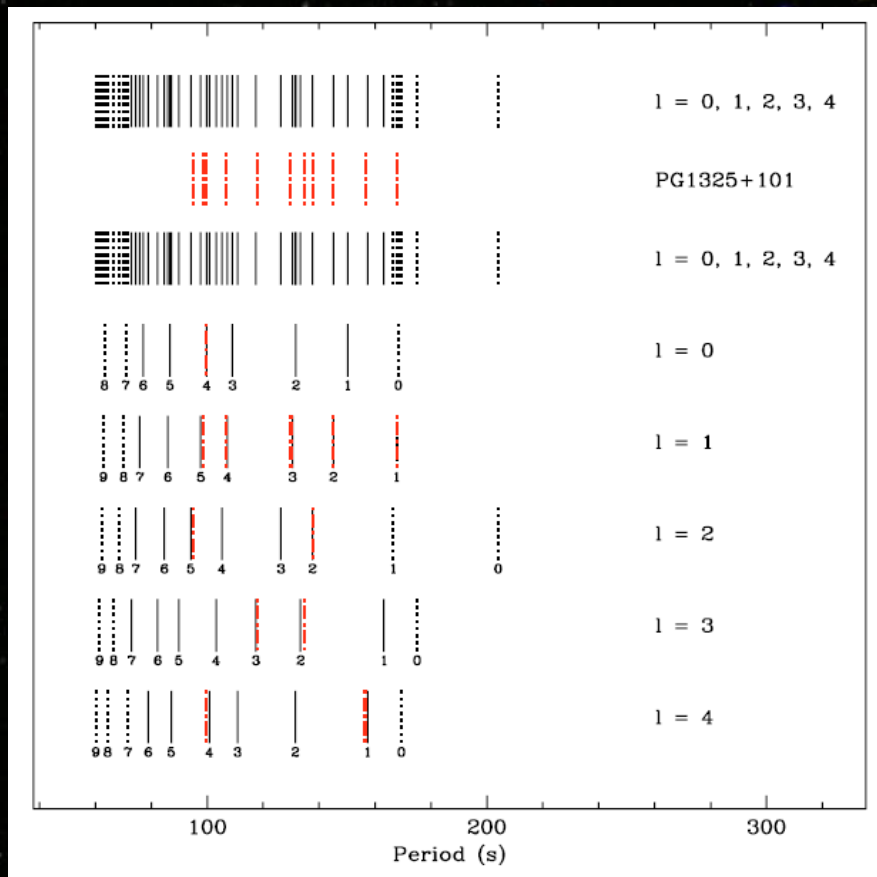
sdB pulsators: Pulsation model fits

'Forward method': Two stage
double optimisation procedure

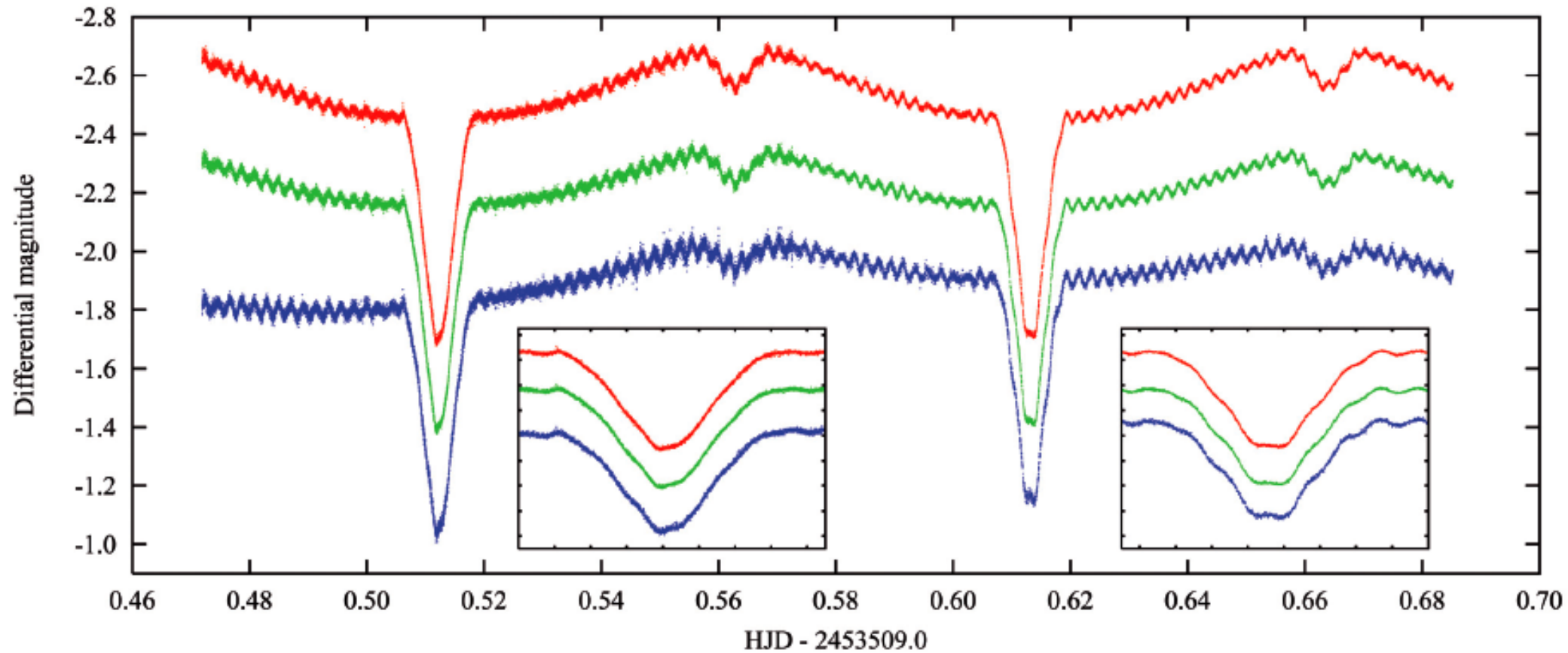
1) In pulsation period domain, finding
the best simultaneous match to all
the observed periods using a merit
function of the form

$$S^2 = \sum_{i=1}^n (P_{\text{obs}}^i - P_{\text{th}}^i)^2,$$

2) The merit function S^2 is minimised
as a function of the model parame-
ters T_{eff} , $\log g$, total mass M , and en-
velope mass fraction $q(\text{H})$
Combined with observational con-
straints from spectroscopy, an opti-
mal solution can be found



NY Vir: The 'rosetta stone'



Single lined eclipsing binaries

Effective temperature and surface gravity can be determined from spectroscopy

The period, inclination angle, and relative radii of the two stars are well determined from the eclipse light-curves

K_1 is the projected velocity of the primary, observed in spectroscopy

We can then derive the following functional equations:

$$a_1 = 0.019757 K_1 \frac{P}{\sin i} [R_{sun}]$$

$$R_1 = r_1 a_1 \left(1 + \frac{1}{q}\right) [R_{sun}]$$

$$M_1 = \left(\frac{K_1}{\sin i}\right)^3 \left(1 + \frac{1}{q}\right)^2 \frac{P}{q}$$

Using these equations we can plot M_1 and R_1 as a function of q

Add the relationship between surface gravity and mass/radius:

$$g = 27360 \frac{M_1}{R_1^2}$$

NY Vir: The 'rosetta stone'

Table 3. System parameters of the three best model fits to RV data and lightcurves of PG 1336–018. The formal 1σ error on the last digit of each parameter is given in parentheses.

Free parameter	Model I	Model II	Model III
$a [R_\odot]$	0.723(5)	0.764(5)	0.795(5)
q	0.282(2)	0.262(2)	0.250(2)
$i [^\circ]$	80.67(8)	80.67(8)	80.67(8)
Ω_1	5.50(3)	5.48(3)	5.47(3)
Ω_2	2.77(1)	2.68(1)	2.62(1)
A_2	0.92(3)	0.92(3)	0.93(3)
$x_2 (g')$	0.38(8)	0.39(8)	0.38(8)
$x_2 (r')$	0.88(8)	0.89(8)	0.89(8)
Derived parameters:			
$M_1 [M_\odot]$	0.389(5)	0.466(6)	0.530(7)
$M_2 [M_\odot]$	0.110(1)	0.122(1)	0.133(2)
$R_1 [R_\odot]$	0.14(1)	0.15(1)	0.15(1)
$R_2 [R_\odot]$	0.15(1)	0.16(1)	0.16(1)
$\log g_1 [\text{cm/s}^2]$	5.74(5)	5.77(6)	5.79(7)
$\log g_2 [\text{cm/s}^2]$	5.14(5)	5.14(5)	5.14(5)
Roche radii: [in units of orbital separation]			
r_1 (pole)	0.191	0.191	0.191
r_1 (point)	0.193	0.193	0.193
r_1 (side)	0.192	0.192	0.192
r_1 (back)	0.193	0.193	0.193
r_2 (pole)	0.198	0.197	0.197
r_2 (point)	0.213	0.215	0.216
r_2 (side)	0.201	0.201	0.201
r_2 (back)	0.210	0.211	0.211
Errors on residuals:			
$\sigma(g')$ [mag]	0.03055	0.03054	0.03057
$\sigma(r')$ [mag]	0.01325	0.01321	0.01321
$\sigma(\text{RV}) [\text{km s}^{-1}]$	8.39	8.39	8.39

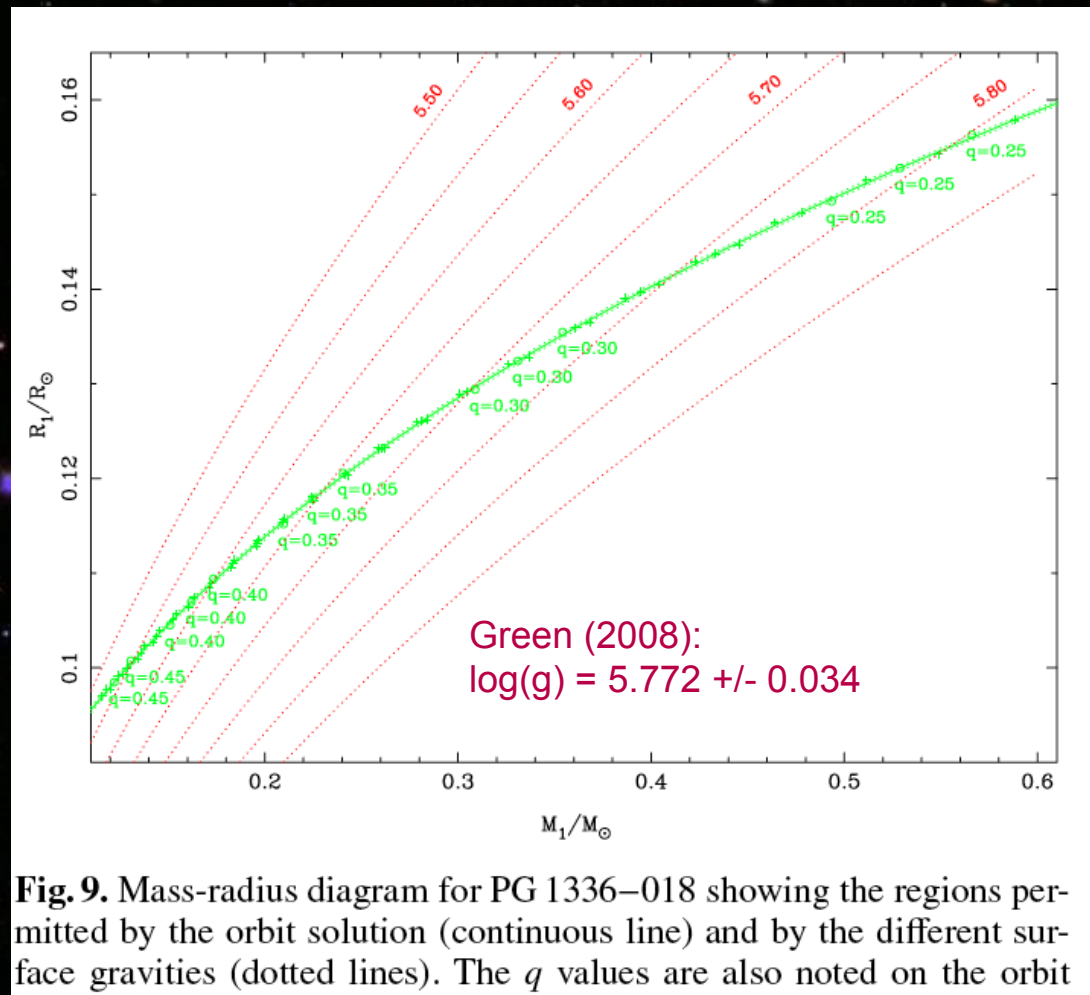
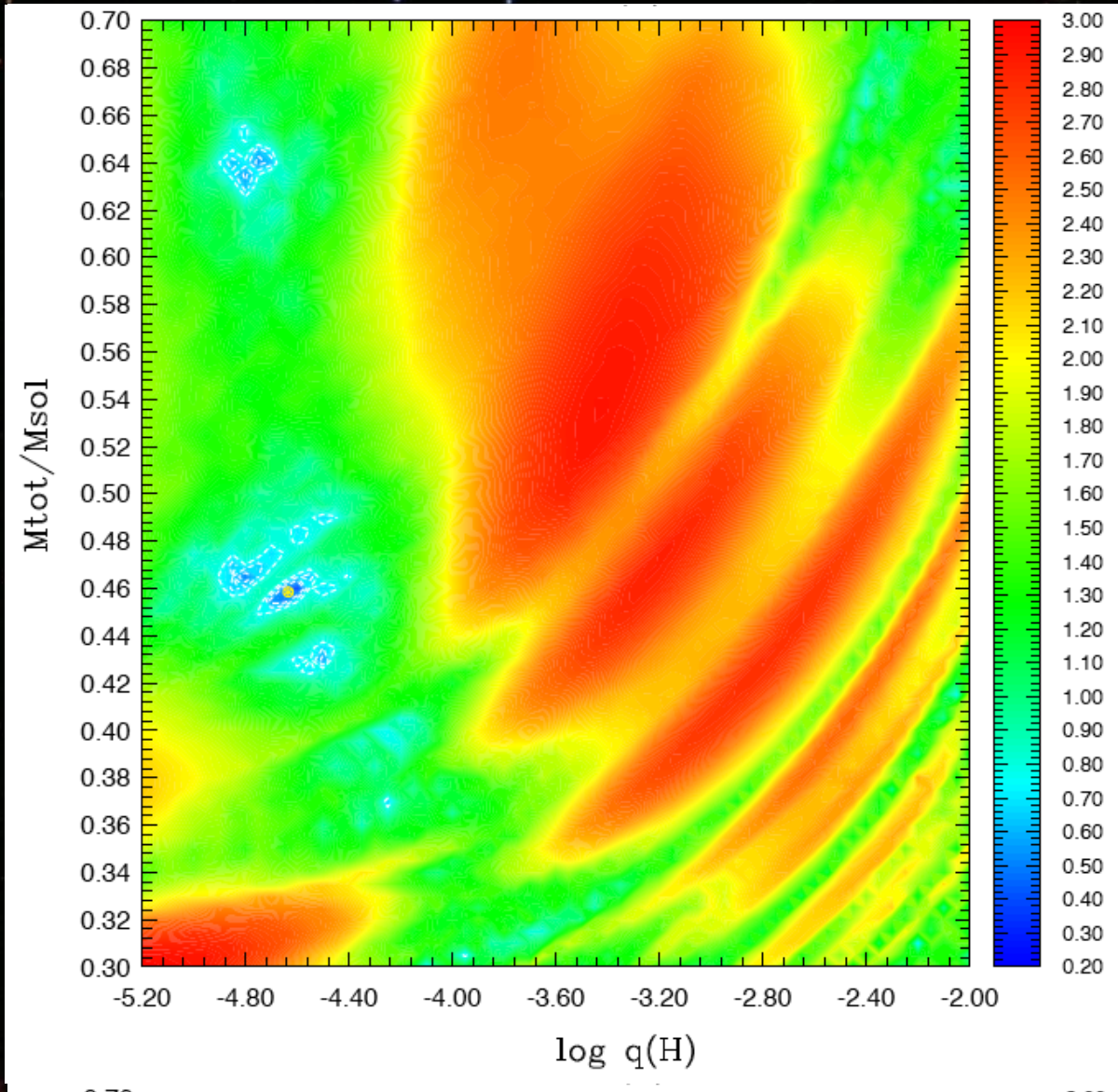


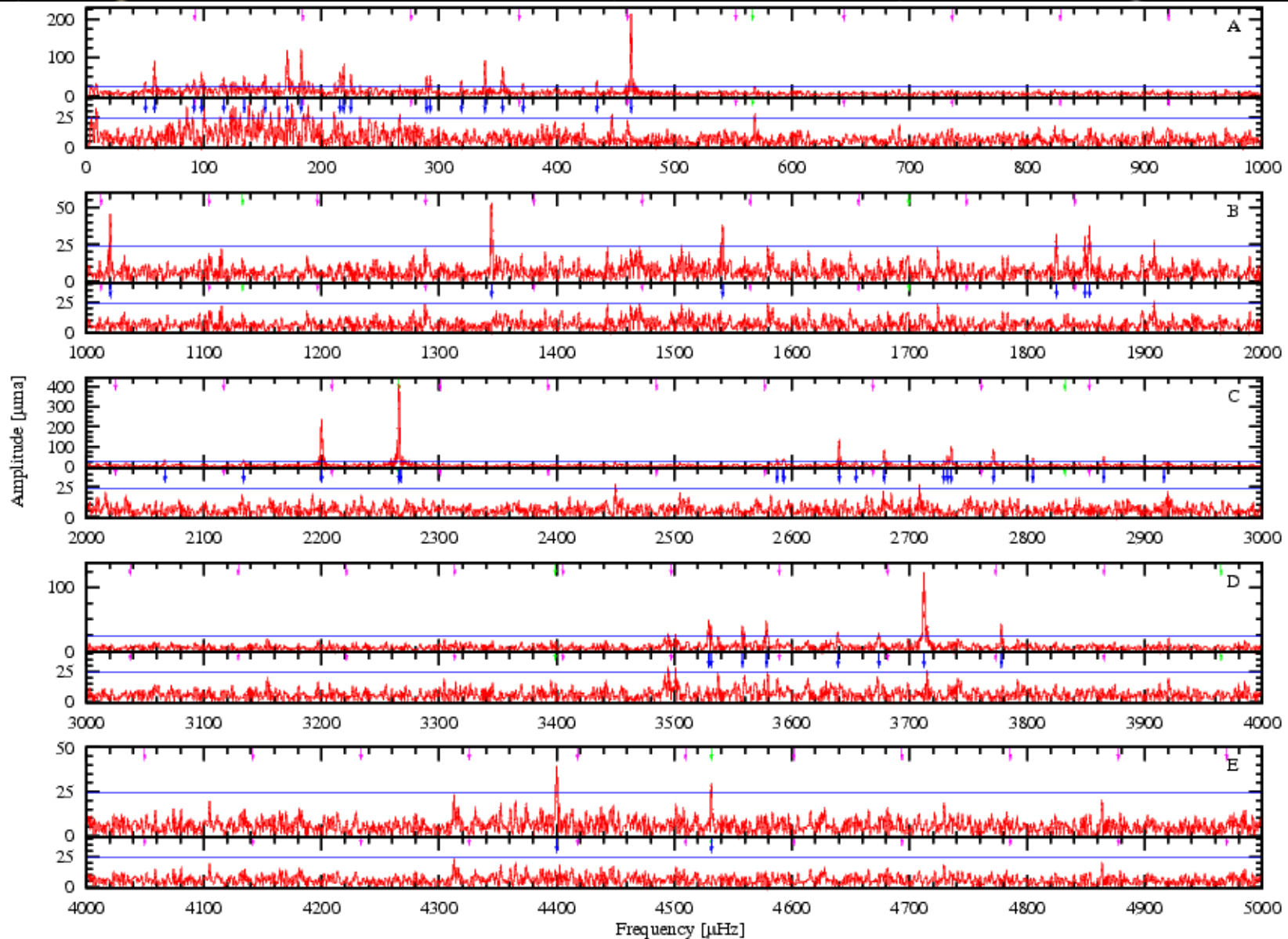
Fig. 9. Mass-radius diagram for PG 1336–018 showing the regions permitted by the orbit solution (continuous line) and by the different surface gravities (dotted lines). The q values are also noted on the orbit

NY Vir: The 'rosetta stone'

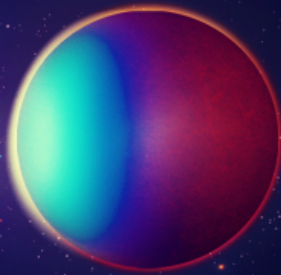


	P_{th} (s)	$\Delta X/X$ (%)	ΔP (s)	Δv (μHz)	Ampl. (%)	Com
	171.5874	
00	183.8524	+0.0694	+0.1276	-3.773	0.20	f_5
	162.7793	-0.3262	-0.5293	+20.041	0.05	f_{28}
	165.7813	
00	168.8961	+0.0792	+0.1339	-4.689	0.10	f_{11}
	179.0037	+0.0147	+0.0263	-0.820	0.40	f_2
00	182.6811	+0.0596	+0.1089	-3.260	0.06	f_{22}
00	186.5128	-0.1465	-0.2728	+7.854	0.37	f_3
	135.1015	
	137.1649	
	139.2924	
00	141.4870	-0.0474	-0.0670	+3.347	0.13	f_9
	143.7518	
	149.7560	
	152.1941	
	154.7129	
	157.3165	
	160.0092	
00	174.1275	-0.2519	-0.4375	+14.466	0.47	f_1
00	177.5890	+0.1748	+0.3110	-9.844	0.07	f_{20}
00	181.1909	+0.0436	+0.0791	-2.409	0.10	f_{12}
00	184.9419	+0.1124	+0.2081	-6.077	0.06	f_{25}
	188.8515	

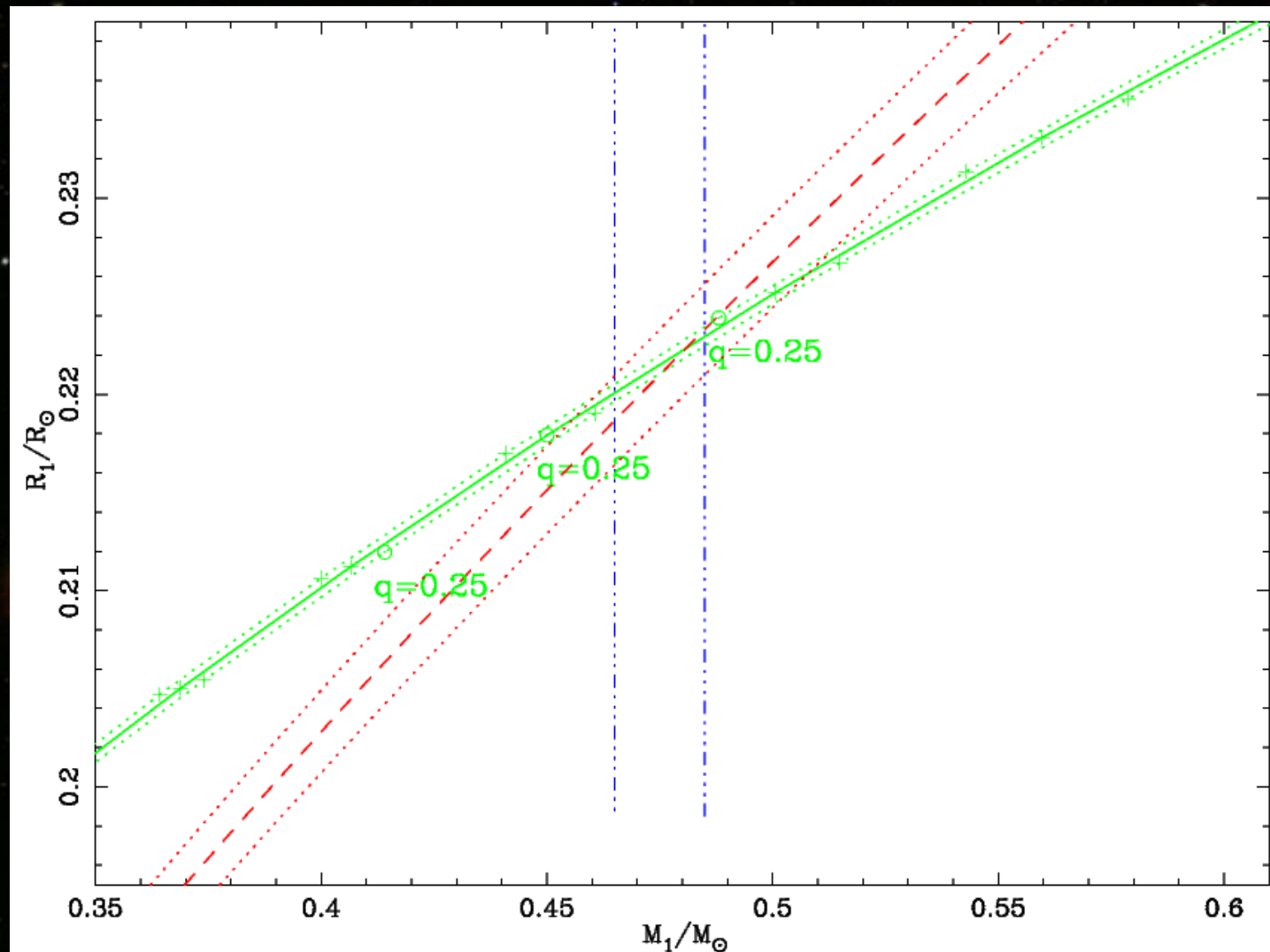
2M 1938+4603 = KIC 9472174



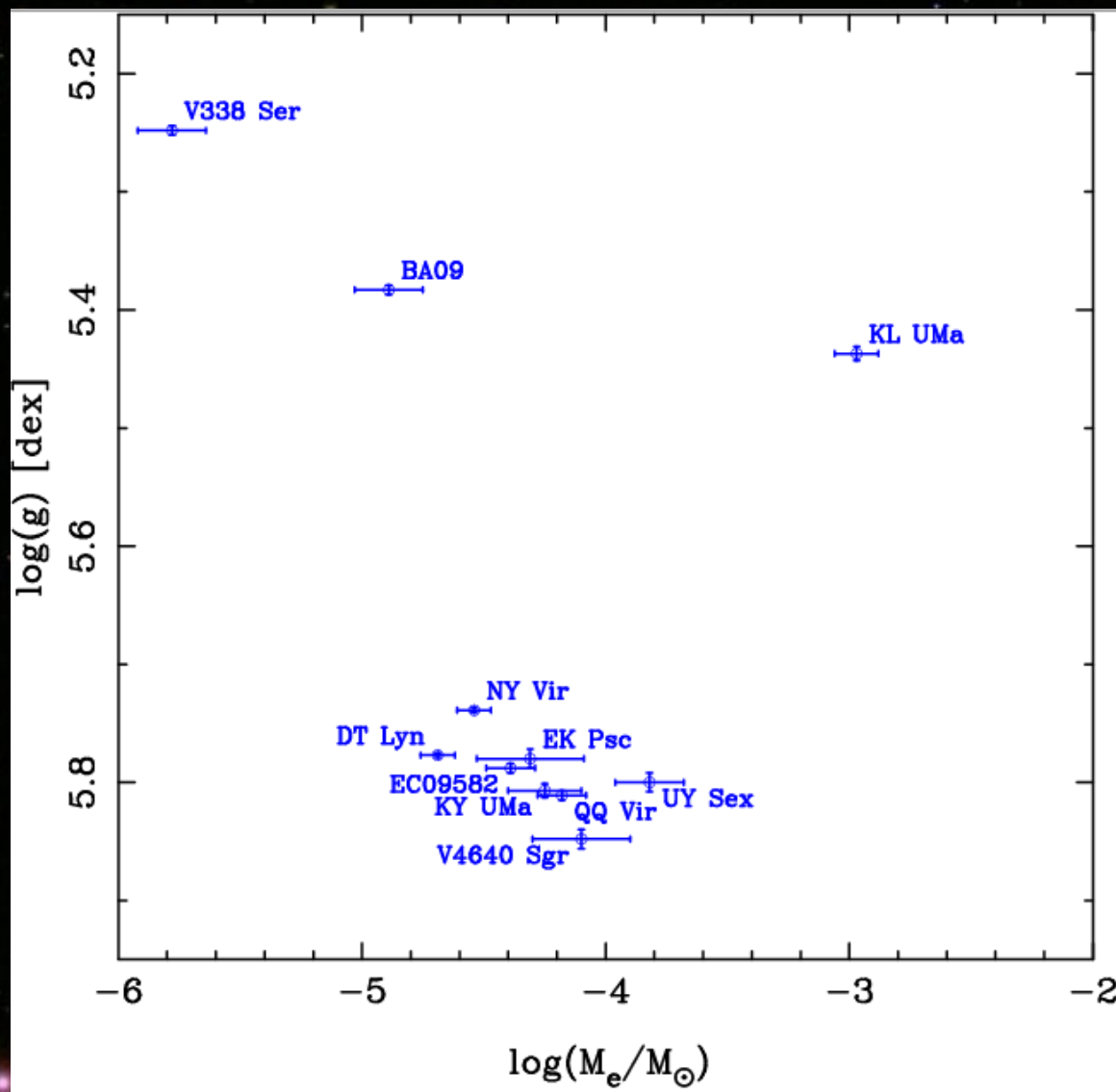
2M 1938+4603 = KIC 9472174



2M 1938+4603 = KIC 9472174



Asteroseismology on the EHB



11 stars with asteroseismology solution using the 'forward method'

Correlation between gravity and envelope mass fraction is unclear

Progress in observations

- ★ **Main objection to the frequency matching method:**
- ★ Models can only match observed frequencies to a precision of a few %
- ★ Models say nothing about the amplitudes of the modes

- ★ **More work on theoretical models are required to bring the models up to the precision of the observations, in particular for g-mode pulsators**
- ★ Requires non-adiabatic pulsation models to be connected to fully evolutionary models for sdB stars
- ★ Evolutionary models must include gravitational settling and radiative levitation

Mode ID from frequency spectra

Advantages:

Works well on faint stars, but requires a rich pulsation spectrum.

- * Multi-site campaigns can provide high frequency resolution and detect low amplitude modes.
- * Kepler space data has changed the game completely!

Problems:

Often, no unique solution for a particular mode is found, because modes with different l 's can be found within the precision of the fit

Mode ID from time-resolved spectroscopy

Advantages:

Possible to make unique mode-ID of a single pulsation period from phase diagrams, but requires high S/N and rotation to break degeneracies

Problems:

Very difficult to get the required S/N on the faint sdBs
Requires phase folding of extended time series
In multi-mode pulsators interference between the modes produce broadening in the phase folded line profiles
Only feasible on a few high amplitude pulsators

Spectroscopic line profile fitting

CCF profiles and model profiles



Table 4. Results of fits to the CCF profile variations. Listed are the best fits, with reduced χ^2 within $[\chi_{\min}^2, \chi_{\min}^2 + 1]$, and below the separation the best fits for every $(\ell=2, |m|\leq\ell)$ combination. Inclination angle is given in degrees, the velocity amplitudes V_p and A_{M_1} in km/s, and the line-broadening σ_G in km/s.

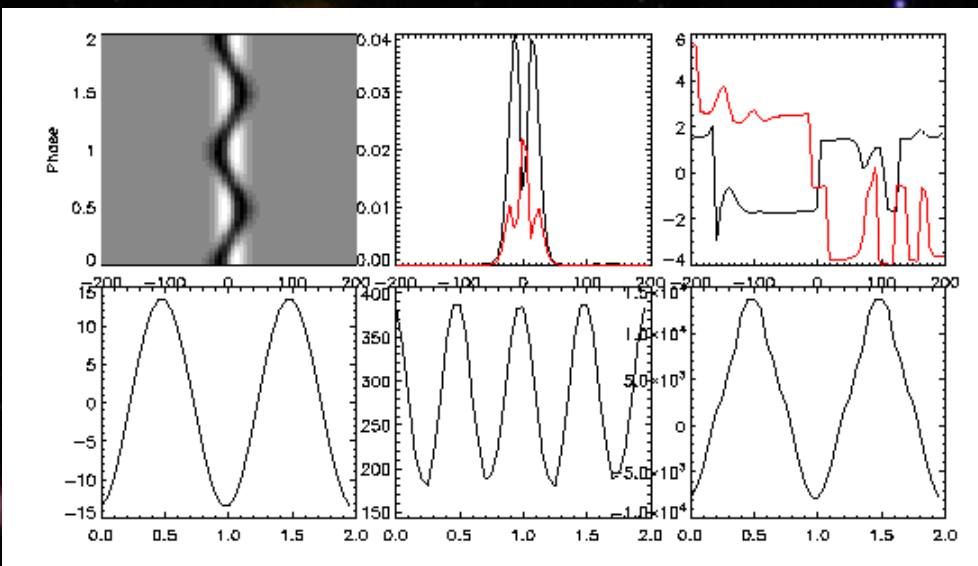
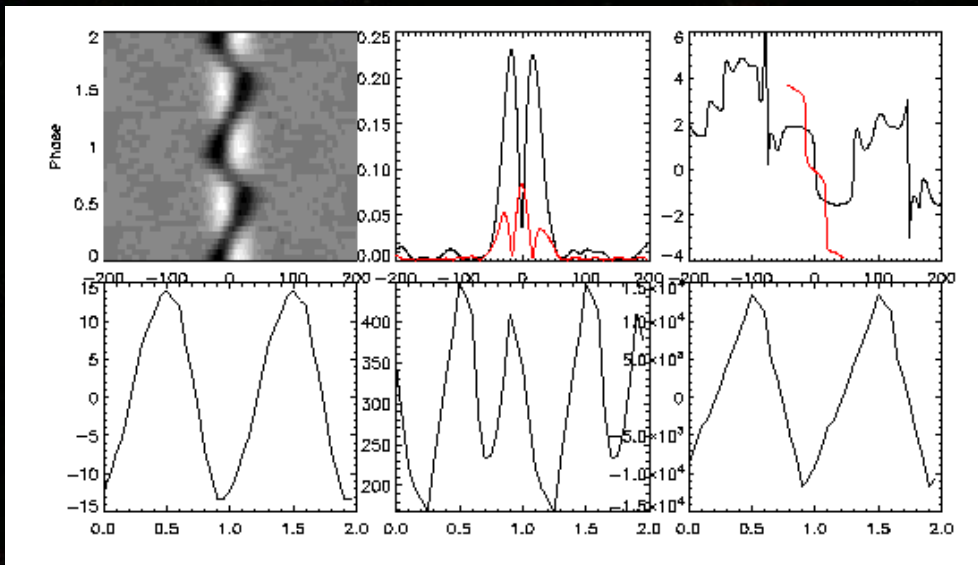
ℓ	m	i	V_p	σ_G	χ^2	A_{M_1}
1	-1	50	35.1 ± 0.1	18.06 ± 0.07	1.62	14.59
1	-1	60	31.3 ± 0.1	19.31 ± 0.06	1.62	14.69
1	-1	70	28.8 ± 0.1	19.96 ± 0.05	1.64	14.71
1	-1	80	27.5 ± 0.1	20.28 ± 0.05	1.65	14.71
1	-1	40	40.3 ± 0.1	16.05 ± 0.08	1.79	14.06
0	0	any	21.5 ± 0.1	22.60 ± 0.04	1.91	14.66
1	0	10	27.3 ± 0.1	21.94 ± 0.04	2.00	14.58
1	0	20	28.5 ± 0.1	21.84 ± 0.04	2.02	14.55
1	0	30	30.8 ± 0.1	21.64 ± 0.05	2.09	14.47
1	0	40	34.4 ± 0.1	21.32 ± 0.05	2.25	14.29
1	1	80	27.2 ± 0.1	20.57 ± 0.05	2.31	14.55
1	1	70	28.5 ± 0.1	20.28 ± 0.05	2.34	14.53
1	1	60	30.8 ± 0.1	19.70 ± 0.06	2.40	14.48
1	1	50	34.5 ± 0.1	18.63 ± 0.06	2.53	14.34
2	-1	40	37.6 ± 0.1	14.74 ± 0.10	4.20	12.09
2	0	10	40.1 ± 0.2	20.43 ± 0.05	4.75	12.49
2	1	50	38.0 ± 0.1	16.27 ± 0.09	5.12	12.19
2	-2	80	35.1 ± 0.1	14.40 ± 0.10	5.27	11.09
2	2	80	34.7 ± 0.1	15.08 ± 0.11	6.53	10.98

- *From a dataset of 842 NOT/FIES R=25.000 spectra
- *Phase folding on the main mode, and cross-correlating 56 metal lines produces sufficient S/N to constrain the mode
- *Simple line profiles, modelling only the surface velocity field, were fitted to the observed profiles

Fig. 5. Observed profiles with the mean amplitude 22 and amplitude 38

Spectroscopic line profile fitting

Balloon 090100001



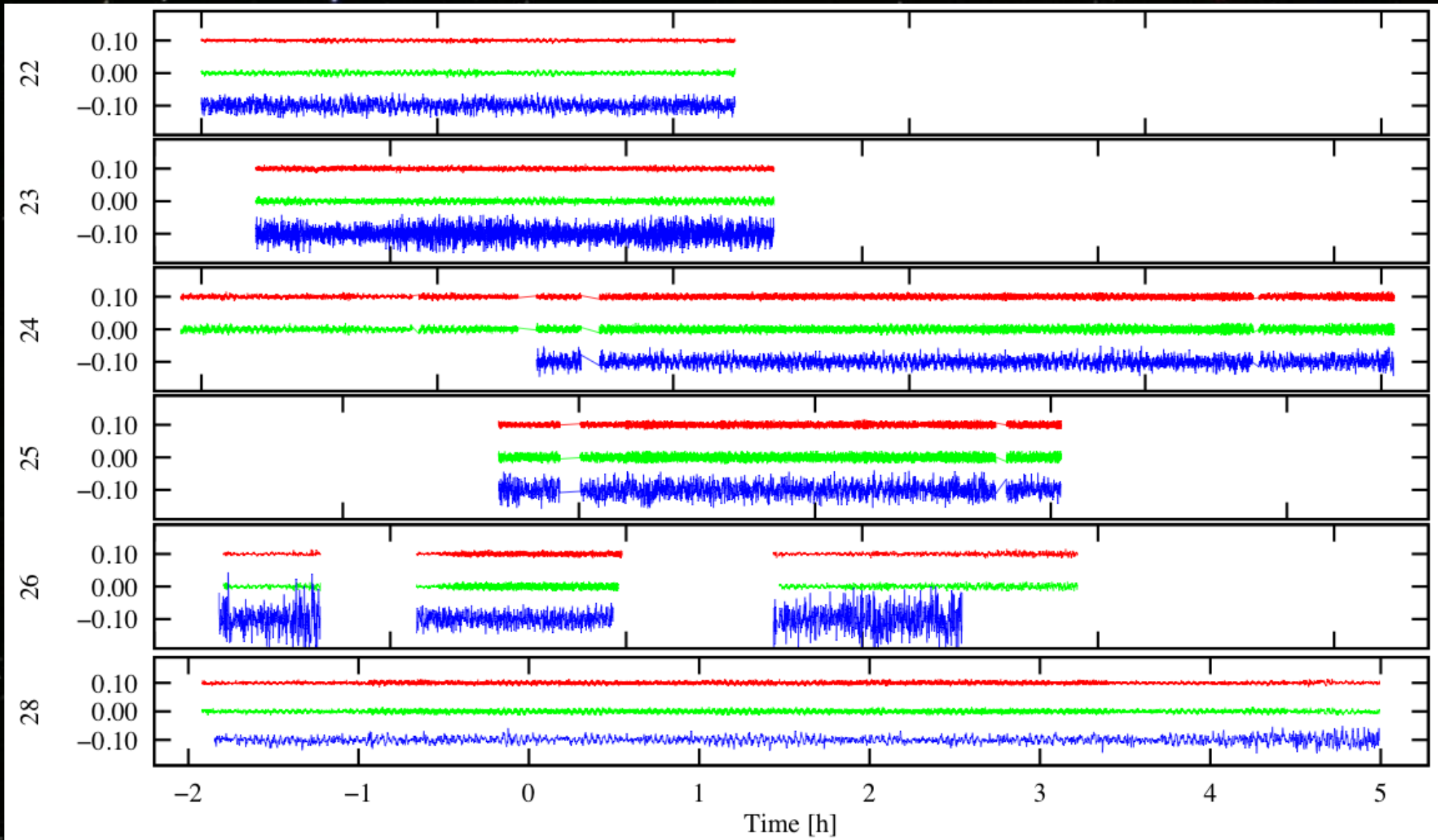
- * Use the full NOT/FIES dataset with 1606 spectra
- * Computes moments from the observed mode
- * Synthetic line profiles generated with BRUCE/KYLIE to include temperature and gravity effects

Oreiro et al. (2010)

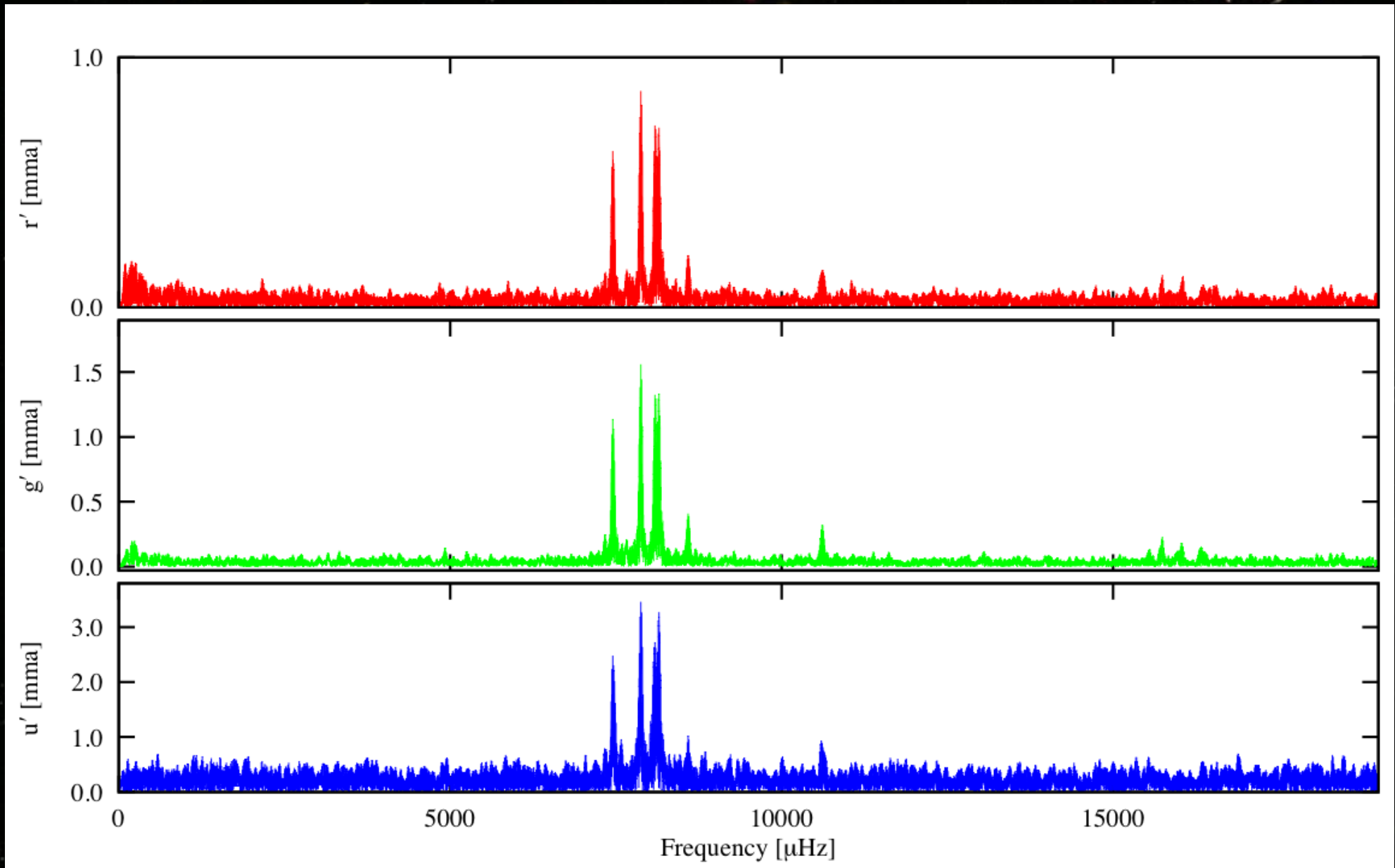
Mode ID from multi-color photometry

- * The amplitude ratio method allows unique mode ID of all modes in a pulsation spectrum
- * Requires very high precision on the amplitudes in order to distinguish between $l=0,1,2$
- * To achieve the required precision, simultaneous observations in several bands are required

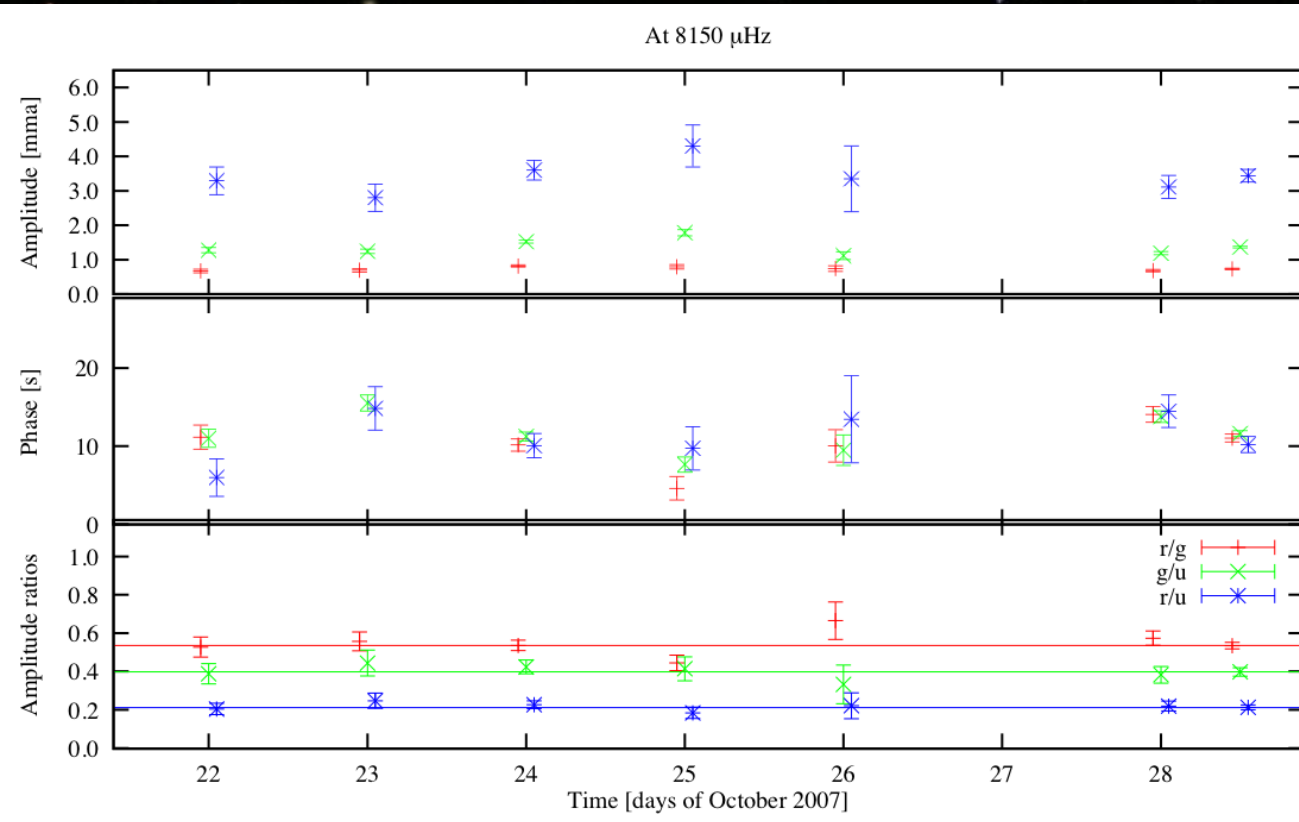
Example: Ultracam on EO Ceti



Example: Ultracam on EO Ceti



Example: Ultracam on EO Ceti

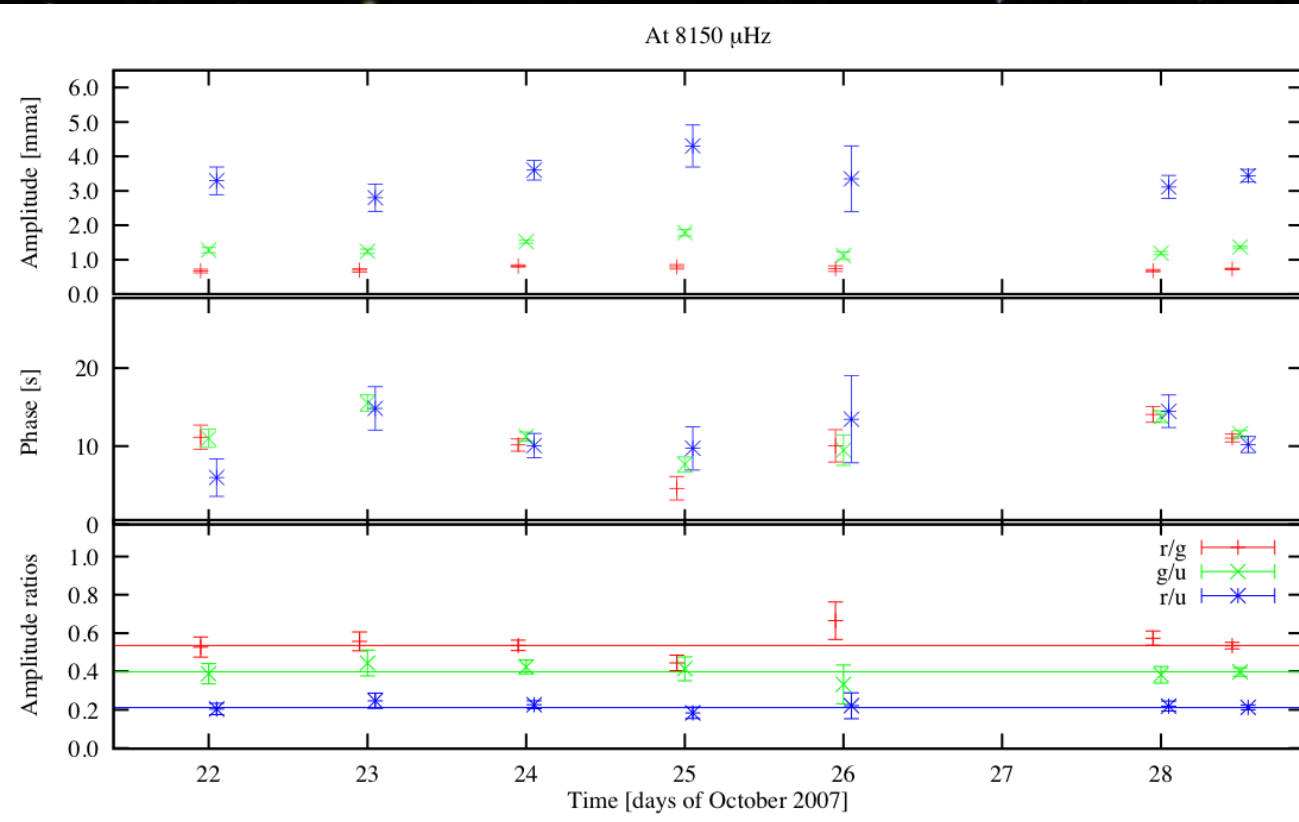


EO Ceti is a composite subdwarf with an F-star companion contributing ~50% of the flux

The observed amplitudes are substantially lower than the intrinsic pulsation amplitudes

The amplitude ratios are affected since the F-star contributes more in the red bands than in the blue

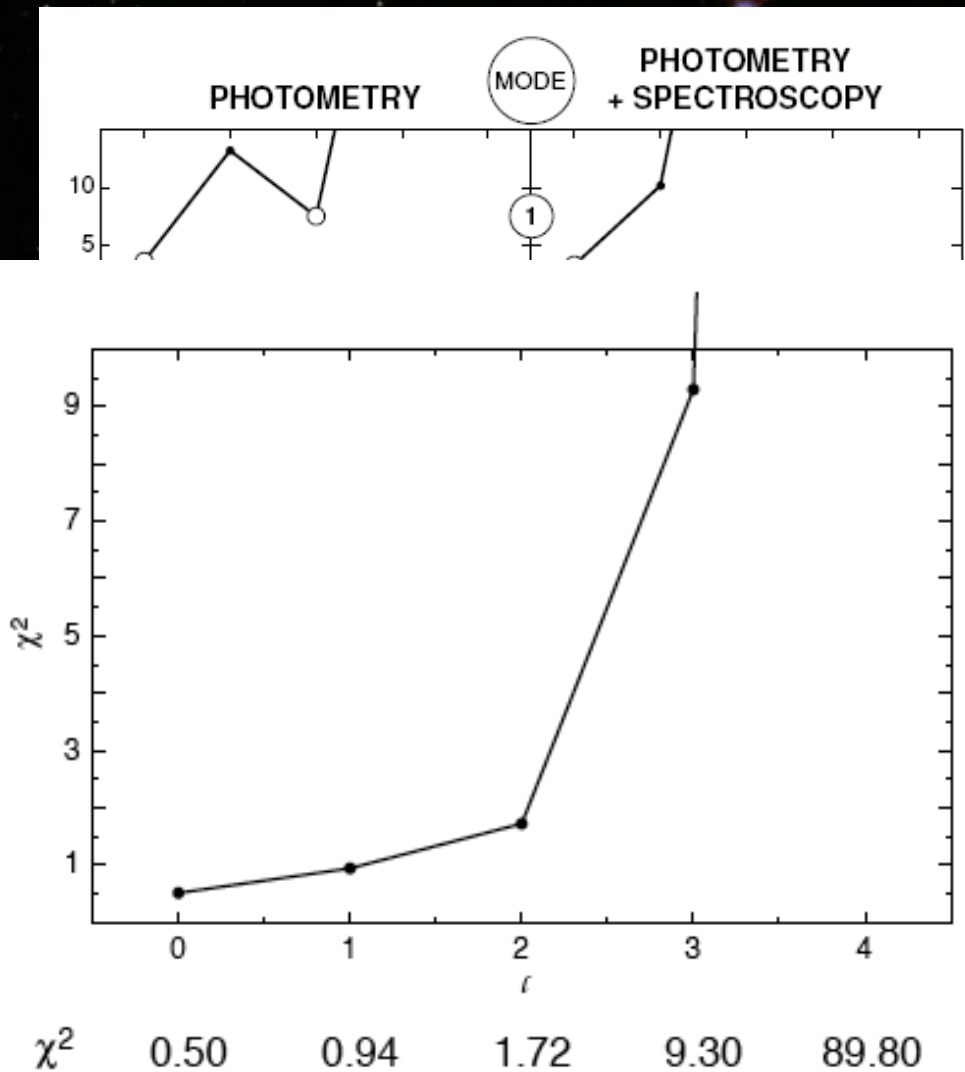
Example: Ultracam on EO Ceti



However, very recently it was found the Hell 4686 line is much stronger than the Hel lines (Østensen 2012). That means that EO Ceti, which was the second sdB pulsator found, is actually an sdO pulsator!

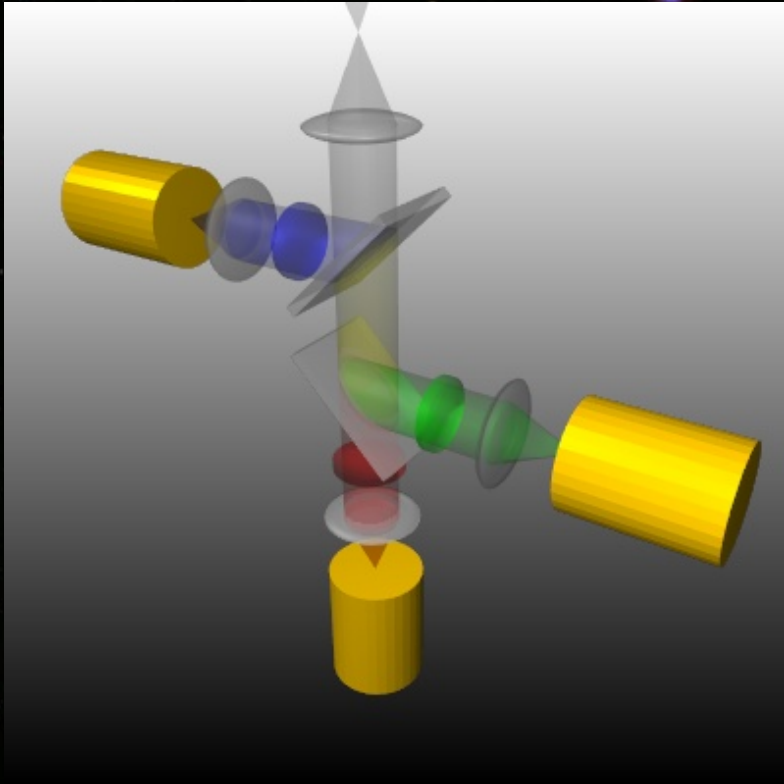
Our sdB models does not apply for sdOs...

Combination method: RV + color



- * Method of Daszyńska-Daszkiewicz et al. 2003 can be used to constrain the degree ℓ
- * Applied to Balloon 090100001 by Baran et al. 2008 ($\ell=0$)
- * To QQ Vir by Baran et al. 2010 ($\ell=0,1$)

Simultaneous 3-band photometry



The key to photometric mode-ID is true simultaneous multi-band photometry

ULTRACAM has shown the way by implementing the key design features:

- * Splitting the light-path with dichroics to obtain simultaneous photometry
- * Fast frame-transfer CCDs to eliminate read-out delays
- * Problem: only small 1024x1024 pixel CCDs

Conclusions

Asteroseismology of EHB stars is progressing fast

Much progress have also been made on evolutionary models, but much still needs to be done

- ★ To explain how single sdB stars loose their envelopes
- ★ To model how the He-flash affects the internal structure

More work is needed to make the pulsation models more sophisticated so that they can

- ★ Fit the observed data to close to the observed precision
- ★ Distinguish different formation scenarios

Why do only 10% of the short period candidates pulsate?

We expected to find more low-level p-mode pulsators with Kepler, but ended up with none...